X-ray amorphous components in sedimentary rocks of Gale crater, Mars: Evidence for ancient formation and long-lived aqueous activity

Rebecca J Smith, S M Mclennan, C N Achilles, E Dehouck, B H N Horgan, N. Mangold, E B Rampe, M Salvatore, K L Siebach, V Sun

X-ray amorphous components in sedimentary rocks of Gale crater, Mars: Evidence for ancient formation and long-lived aqueous activity

R. J. Smith[1*], S. M. McLennan[1], C. N. Achilles[2], E. Dehouck[3], B. H. N. Horgan[4], N. Mangold[5], E. B. Rampe[6], M. Salvatore[7], K. L. Siebach[8], and V. Sun[9]

[1]Department of Geosciences, SUNY Stony Brook, Stony Brook, NY 11794, USA

[2]NASA Goddard Space Flight Center, Greenbelt, MD 20771, USA

[3]Université de Lyon, Univ Lyon 1, ENSL, CNRS, LGL-TPE, F-69622, Villeurbanne, France

[4]Department of Earth, Atmospheric, and Planetary Sciences, Purdue University, West Lafayette, IN 47907, USA

[5]Laboratoire de Planétologie et Géodynamique, UMR6112, CNRS, Université de Nantes, France

[6]Astromaterials Research and Exploration Science Division, NASA Johnson Space Center, Houston, TX 77058, USA

[7]Department of Astronomy and Planetary Science, Northern Arizona University, Flagstaff, AZ, 86011, USA

[8]Earth, Environmental and Planetary Sciences, Rice University, TX 77005, USA

[9]Jet Propulsion Laboratory, California Institute of Technology, Pasadena, CA 91109, USA

[*]Corresponding author: Rebecca Smith (rebecca.j.smith@stonybrook.edu)

Key Points:

- X-ray amorphous abundances are positively correlated with SiO_2 content, and amorphous SiO_2 and FeO_T contents are anticorrelated.
- X-ray amorphous SiO_2 and FeO_T contents in Gale crater sedimentary rocks largely represent multiple aqueous processes occurring over time.
- It is unclear how such metastable materials have persisted for billions of years.

Abstract

The CheMin instrument on the Mars Science Laboratory rover *Curiosity* detected ubiquitous high abundances (~15-70 wt%) of X-ray amorphous components (AmCs) in ancient sedimentary rocks of Gale crater. Mechanisms and timing of formation for the AmCs are poorly constrained, and could include volcanic, impact, or aqueous processes. We explore trends in AmC composition and abundance, and look for systematic compositional variation between sites within Gale crater. AmC compositions were estimated indirectly based on bulk chemistry and the nature and abundance of the crystalline phases for 19 sedimentary rock samples. AmC abundances positively correlate with AmC SiO_2 contents, and a mixing relationship appears to exist between SiO_2-rich and FeO_T-rich AmC endmembers. Endmember compositions are inconsistent with volcanic or impact glass alone, and so we conclude that the SiO_2 and FeO_T contents formed largely through aqueous processes. Cross-cutting relationships and geologic context provide evidence that the most SiO_2-rich AmCs observed in Gale crater thus far may result from interactions with localized fluids during late diagenesis. AmCs with moderate to low SiO_2 contents likely formed earlier (before or soon after the deposition of sediments). Thus, the AmC SiO_2 and FeO_T contents in Gale crater rocks represent mixtures of sedimentary materials formed over most of the sedimentary history of Gale crater, starting before the first sediments were deposited in the crater (late Noachian), and ending well after the youngest sediments were lithified (at least mid Hesperian). However, it remains unclear how these metastable minerals have persisted through billions of years of diagenesis in Gale crater sediments.

Plain Language Summary

The CheMin instrument on the Mars Science Laboratory rover *Curiosity* detected ubiquitous high abundances (~15-70 weight %) of amorphous materials in ancient sedimentary rocks of Gale crater. It is uncertain what geologic processes these materials represent (volcanic eruptions, impacts, or interactions with water), and when these materials were formed. Here we explore these possible formation mechanisms and their timing by estimating the chemical compositions of the amorphous materials, and looking for trends and variations in their compositions along the rover traverse. We find that amorphous iron- and silica-rich materials formed mostly through interactions with water, and likely represent mixtures of chemical weathering products, chemical sediments, and cements that accumulated over time. We also find that some of the amorphous materials formed early on in the history of the crater, while others formed long after sediments were deposited and turned into rock, indicating that water persisted at Gale crater for ~1 billion years. On Earth, it is thought that amorphous materials are readily converted into more crystalline materials in the presence of water, but it is unclear why this is not the case for Mars.

1 Introduction

The Mars Science Laboratory (MSL) rover *Curiosity* has examined hundreds of stratigraphic meters of ancient fluviolacustrine and eolian sedimentary rocks in Gale crater (137.4°E, -4.6°N) since landing in August 2012 (Grotzinger et al., 2015; Figure 1). Among the most puzzling discoveries is the detection of high abundances (~15-70 wt%) of X-ray amorphous components (AmCs) in all sedimentary materials analyzed, including both unconsolidated eolian sediments and ancient (~3.5 billion-year-old) sedimentary rocks (Rampe et al., 2020a and references therein). Addressing the mechanisms and timing of formation of these components is critical for understanding Martian sedimentary processes, but they remain largely unconstrained

(McLennan et al., 2019). Amorphous materials could include primary glass deposited by fluvial or eolian processes (e.g., ash fall, impact glasses), secondary alteration products, chemical precipitates from surface or pore waters, and/or post-depositional diagenetic products. For some of the sampling locations, evolved gas analyses measured by the Sample Analysis at Mars (SAM) instrument show wide volatile release temperatures for H_2O and SO_2 that have been partially attributed to X-ray amorphous materials, suggesting that at least some fraction of the X-ray amorphous components formed through aqueous processes (Leshin et al., 2013; Sutter et al., 2017).

AmCs were detected with the CheMin X-ray diffractometer (XRD) (Blake et al., 2012). CheMin analyses are restricted to sieved sediment or powdered drill fines. As of December 2019 (sol 2300), CheMin data are available for 19 sedimentary rock samples along the rover traverse, representing each of the major stratigraphic units encountered (Figure 1).

Such high abundances of X-ray amorphous materials in 3-4 Gy old and diagenetically altered sedimentary rocks is an unexpected discovery, as amorphous and nanocrystalline materials are thermodynamically metastable and are susceptible to particle coarsening processes that convert amorphous and nanocrystalline materials to more stable minerals and larger crystals (e.g., Steefel and Van Cappellen, 1990; De Yoreo et al., 2015). Therefore, it is widely thought that they should not be found in high abundance in sedimentary rocks, which undergo diagenesis before, during, and after lithification (Mack et al., 1993; Harsh, 2005). For example, the oldest known occurrences of opaline silica are Cretaceous in age, but it is exceedingly rare to find opaline silica in terrestrial sedimentary rocks older than a few million years (e.g., Tosca and Knoll, 2009). Yet, amorphous and nanocrystalline weathering products are significant components (~10-30 wt%) of 30-50 My old Mars-analog paleosols (Smith et al., 2018), indicating that this general conclusion might not always hold true, and that some settings allow amorphous materials to be preserved in Earth sediments for at least 10s to 100s of millions of years.

Previous workers estimated bulk AmC compositions in Gale crater through mass balance calculations that combine bulk sample geochemistry from the Alpha Particle X-ray Spectrometer (APXS; Gellert et al., 2015) with CheMin-derived mineral stoichiometries and abundances (Blake et al., 2013; Dehouck et al., 2014; Vaniman et al., 2014; Morris et al., 2016; Treiman et al., 2016; Achilles et al., 2017, 2020; Rampe et al., 2017; Yen et al., 2017). These results show that AmC compositions vary between sampling locations, particularly in SiO_2 and FeO_T abundance. However, to date, no study has explored if there are any trends with AmC composition and abundance, or explored if there is systematic compositional variation between sedimentary units in Gale crater. Here we focus on AmC SiO_2 and FeO_T concentrations and examine how the proportions of these two oxides are related to AmC abundances and stratigraphic position. We then place observations into the context of our current understanding of the geologic history of Gale crater.

2 Geologic Overview

The ~154 km diameter impact basin Gale crater is located near the equator of Mars, on the crustal dichotomy boundary between the northern lowlands and the southern highlands. As of sol (one day on Mars) 2300, MSL had driven over 20 km laterally and gained 380 m of elevation. Almost all rocks that MSL has encountered have been sedimentary, and the strata are generally flat-lying such that elevation can be used as a proxy for thickness of the stratigraphic

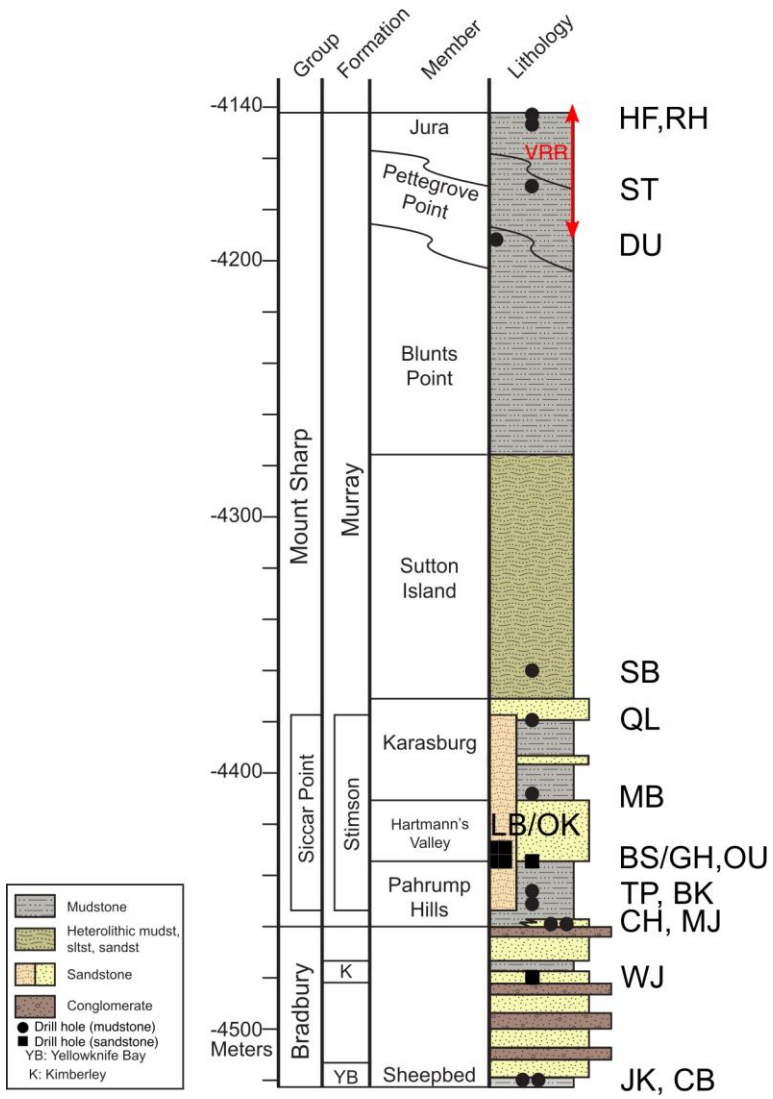

Figure 1. Stratigraphic column of Gale crater (up to sol 2300). Drill holes: JK–John Klein, CB–Cumberland, WJ–Windjana, CH–Confidence Hills, MJ–Mojave, TP–Telegraph Peak, BK–Buckskin, OU–Oudam, MB–Marimba, QL–Quela, SB–Sebina, DU–Duluth, ST–Stoer, HF–Highfield, RH–Rockhall, BS–Big Sky, OK–Okoruso, GH–Greenhorn, LB–Lubango. Stratigraphic position of Vera Rubin ridge (VRR) is shown near the top. Figure credit: the MSL Science Team sed/strat working group.

section. Along its traverse, the rover has observed and investigated approximately 380 m of sedimentary rock stratigraphy comprising the crater plains and the central mound Mount Sharp (Aeolis Mons) that rises ~5 km high from the floor of Gale crater (e.g., Grotzinger et al., 2014, 2015).

The Gale crater impact event occurred ~3.6 to 3.8 Gy ago during the late Noachian/early Hesperian epochs (Thomson et al., 2011). Based on careful documentation of the lithologies encountered along the rover traverse, the rock-forming sediments were supplied to Gale crater by

a combination of fluvial, lacustrine, and eolian processes (Figure 1; Edgar et al., 2017; Williams et al., 2013; Grotzinger et al., 2014, 2015; Rivera-Hernández et al., 2020; Stack et al., 2019; Banham et al., 2018). It is possible that the entire crater was filled with sediments by the late Noachian/early Hesperian before being eroded through eolian processes (Malin and Edgett, 2000; Le Deit et al., 2013; Grotzinger et al., 2015). Further sedimentation, evidenced by the unconformable eolian Stimson formation (Watkins et al., 2015, Banham et al., 2018) was followed by additional eolian erosion to form the modern crater topography, likely approaching the modern topography approximately 3 billion years ago (Grant et al., 2014).

Multiple diagenetic events are recorded in the sedimentary rocks in Gale crater, but other than a K-Ar age date <3 Ga (possibly as young as ~2.1 Ga) for likely jarosite in a single drill hole location (Martin et al., 2017), the timeframes for these processes are poorly constrained. Buried sediments underwent the diagenetic process of lithification, which includes porosity reduction through compaction and cementation (Worden and Burley, 2003), and contain evidence for more localized early diagenetic processes including concretions, desiccation and syneresis cracks, and lenticular crystal pseudomorphs (Siebach et al., 2014; Stack et al., 2014; Stein et al., 2018; Sun et al., 2019; Blaney et al., 2014; Kah et al., 2018). Extensive networks of Ca-sulfate veins and fracture-associated alteration halos suggest that diagenetic fluids continued to circulate through the rocks long after lithification (e.g. Nachon et al., 2014, 2017; Frydenvang et al., 2017; Yen et al., 2017; Gabriel et al., 2019; Kronyak et al., 2019).

At the time of this study, MSL has examined three major stratigraphic groups (Figure 1). The Bradbury group rocks, comprising mostly fluviodeltaic sediments, make up part of the crater floor deposits, and are interpreted to be the oldest rocks examined by the rover (Grotzinger et al., 2015). CheMin examined three Bradbury group drill hole locations: two lacustrine mudstones in the Yellowknife Bay formation, John Klein (JK) and Cumberland (CB) (see Figure 1 caption for sample name abbreviations used throughout the text), and one sandstone consisting of reworked deltaic and eolian sediments located in the Kimberley formation, Windjana (WJ) (Rice et al., 2017; Vaniman et al., 2014; Treiman et al., 2016; Morrison et al., 2018). The Bradbury group rocks likely had Fe-rich olivine tholeiitic sediment sources (JK and CB) with the possibility of an additional alkali-feldspar-rich sediment source in some locations (WJ) (e.g., Treiman et al., 2016; Edwards et al., 2017; Siebach et al., 2017; Bedford et al., 2018; Payré et al., 2020).

As a whole, the Mount Sharp group overlies the Bradbury group, and all of the Mount Sharp group rocks examined by the rover are thought to be younger than those examined in the Bradbury group (Grotzinger et al., 2015). As of sol 2300, CheMin had analyzed 12 drill hole locations within the Mount Sharp group (Morris et al., 2016; Rampe et al., 2017, 2020b; Achilles et al., 2020). Most of these rocks are fluviolacustrine mudstones and fine-grained sandstones (e.g., Rivera-Hernández et al., 2020) that have geochemical compositions distinct from sediments in the Bradbury group (Berger et al., 2020; Thompson et al., 2020) indicating a change in dominant sediment sources. Mount Sharp group sediment compositions are mostly fractionated, relatively SiO_2-rich subalkaline basalt (Bedford et al., 2018). The Mount Sharp group also includes Vera Rubin ridge (VRR; between ~ -4190 and -4140 m), a topographic ridge that shows strong spectral signatures of hematite from orbit and the ground, and is interpreted to have experienced substantial diagenetic alteration relative to the surrounding units (e.g., Fraeman et al., 2020; David et al., 2020; Horgan et al., 2020; L'Haridon et al., 2020; Rampe et al., 2020b).

Both the Bradbury and Mount Sharp groups were buried, lithified, and later exhumed by eolian erosion (Malin and Edgett, 2000; Grotzinger et al., 2015; Day et al., 2016). Some time

after erosion, the subaerial sand dune sediments of the Siccar Point group were deposited on some sections of the Mount Sharp group (Figure 1). The eolian dunes were then buried and lithified, creating an unconformable surface between parts of the Mount Sharp group and the Siccar Point group (Watkins et al., 2016; Banham et al., 2018). CheMin analyzed four drill holes within the Siccar Point group: two within parent bedrock, Big Sky (BS) and Okoruso (OK), and two within light-toned alteration "halos" surrounding central fractures, Greenhorn (GH) and Lubango (LB) (Yen et al., 2017). The sediments for the Siccar Point group rocks have a subalkaline basaltic composition, and the Siccar Point and Bradbury groups are hypothesized to share a similar local sediment source (Bedford et al., 2020). The fracture-associated alteration halos are silica-enriched zones ~50 cm wide that crosscut both the Mount Sharp and overlying Siccar Point group rocks (Frydenvang et al., 2017; Yen et al., 2017). These alteration halos have been interpreted as late diagenetic features that represent either chemical precipitates (Frydenvang et al., 2017) or leaching residue (Yen et al., 2017), and may have formed as a result of multiple fluid episodes (Yen et al., 2017; Hausrath et al., 2018).

3 Materials and Methods

3.1 Calculating X-ray amorphous component compositions

AmC compositions were determined using mass balance calculations for all rock samples analyzed in the first ~2300 sols of the mission (Figure 1). We used methods developed by Dehouck et al. (2014) and validated using analog samples by Smith et al. (2018), in which we input bulk sample geochemistry from APXS (representing crystalline + amorphous compositions), crystalline mineral abundances and compositions from CheMin, and AmC abundance from CheMin (see Supplemental Material for input details). The crystalline component composition was subtracted from bulk sample composition so what remained was an estimate of the bulk AmC composition, with several caveats listed below. We performed two mass balance calculations for each sample: (1) a "best estimate" composition, named as such because only the best estimate abundance for each mineral was considered during the calculation (i.e., uncertainties on mineral abundances were not considered) resulting in only one AmC composition for each sample, (2) a range of possible AmC compositions using mineral abundance uncertainties (see Dehouck et al., 2014 for details). Here we focused on "best estimate" compositions, and note that the ranges for AmC SiO_2 and FeO_T were mostly < ±5 wt% (Table S1). Compositions were reported as oxide wt% in 100% AmC (Table S2), as opposed to wt% oxide in the amorphous state in 100% sample (crystalline + AmC), because we are interested in how the composition (SiO_2 and FeO_T content) of the amorphous material changes between locations.

APXS frequently acquires multiple bulk sample geochemistry measurements of drilled samples (e.g., drill tailings, discard pile). We used measurements of post-sieve dump piles when available or fines dumped from the drill bit to be most consistent with samples measured by CheMin (Table S3). Crystalline mineral abundances and compositions are from CheMin XRD pattern Rietveld refinements (Morrison et al., 2018; Achilles et al., 2020; Rampe et al., 2020b; Tables S4-5). Opal-CT, identified in four samples (TP, BK, OU, HF; Rampe et al., 2020a; see Figure 1 for sample name abbreviations), was included in the AmC. Clay minerals were included in the crystalline component, and abundances and compositions were based on FULLPAT analyses and XRD pattern comparisons (Tables S6-S7; Bristow et al., 2015, 2018; Baudat et al.,

1992; Brigatti, 1983; Novák and Čícel, 1978; Post, 1984; Treiman et al., 2014). Lastly, we used either the AmC abundance derived from FULLPAT XRD analyses (Morrison et al., 2018; Achilles et al., 2020; Rampe et al., 2020b) or the minimum AmC abundance needed to produce a chemically realistic AmC composition if the XRD-derived abundance resulted in negative AmC oxide abundances (Table S1).

Caveats for interpreting mass balance calculation results include: (1) elements in crystalline phases below the CheMin XRD detection limit of ~1 wt.% (e.g., Cr in chromite, Ti in anatase) are allocated to the AmC composition; (2) minor element substitutions not accounted for in ideal structure formulas for crystalline minerals (e.g., Al, Ti, Cr, Mn, and Na in pyroxenes; K in plagioclase) are also allocated to the AmC composition; (3) when present and poorly constrained, complex clay mineral compositions can affect the accuracy of AmC compositions (Dehouck et al., 2014; Smith et al., 2018). These potential compositional artifacts add additional, but not readily quantifiable, uncertainties, especially for elements at relatively low concentrations in the amorphous component, including Ti, Al, Mn, Na, K, Cl, P, and Cr. Accordingly, this study focuses on SiO_2 and FeO_T because their concentrations in the AmC are relatively high, so uncertainties on abundances, even if a small proportion resides in unaccounted for crystalline phases, are relatively low, and they are both essential compositional constituents in several of the proposed amorphous phases.

4 Results

Calculated SiO_2 and FeO_T contents (wt% oxide in AmC) are compared to AmC abundances in Figures 2a and 2d. Samples with high AmC abundances tend to have SiO_2-rich AmCs, and samples with low AmC abundances tend to have FeO_T-rich AmCs. This correlation is evidence for a mixing relationship between hypothetical SiO_2-rich and FeO_T-rich AmC endmembers.

Linear regression provides an estimate of the composition of the hypothetical SiO_2-endmember (i.e., intercept at FeO_T = 0 wt%), which is not pure SiO_2, but 72.3% (± 8.5%) SiO_2 at 2-standard error with an r^2 value of 0.733. This should be considered a minimum SiO_2 wt% value, because ~2-7 wt% of the oxides in each sample allocated to the AmC composition could actually be present in the crystalline components (TiO_2, MnO, Cr_2O_3, P_2O_5, Cl; Table S2). By subtracting these oxides from each amorphous component, and renormalizing to 100%, we estimate that the SiO_2 wt% value could actually be at high as ~76.0 (± 7.2%) SiO_2 at 2-standard error with an r^2 value of 0.798 (Figure 2c). The improved fit could also be indicative of a better SiO_2 composition estimate. Combined, these estimates (including the 2-standard errors) indicate a SiO_2-rich endmember that is between ~64 and 83 wt% SiO_2. No single oxide shows a positive correlation with AmC SiO_2, so several different constituents are responsible for the impurity of the SiO_2-endmember.

The linear regression in Figure 2 also provides a composition for the hypothetical FeO_T-endmember, which is ~52% FeO_T (at SiO_2 = 0 wt%). It might seem that this composition is predominantly constrained by the most FeO_T-rich AmC drill hole location (WJ), which has a composition very different from all other AmCs. However, if the linear regression is forced to ignore the WJ location (Figure 2b), the change to the hypothetical FeO_T-endmember composition is minimal (~55% FeO_T). Similar to the AmC SiO_2, AmC FeO_T shows no strong positive correlation with any single oxide, and so several different constituents are responsible for the impurity of the FeO_T-endmember.

254 Figure 3 shows stratigraphic variation in AmC abundance and FeO_T and SiO_2 contents

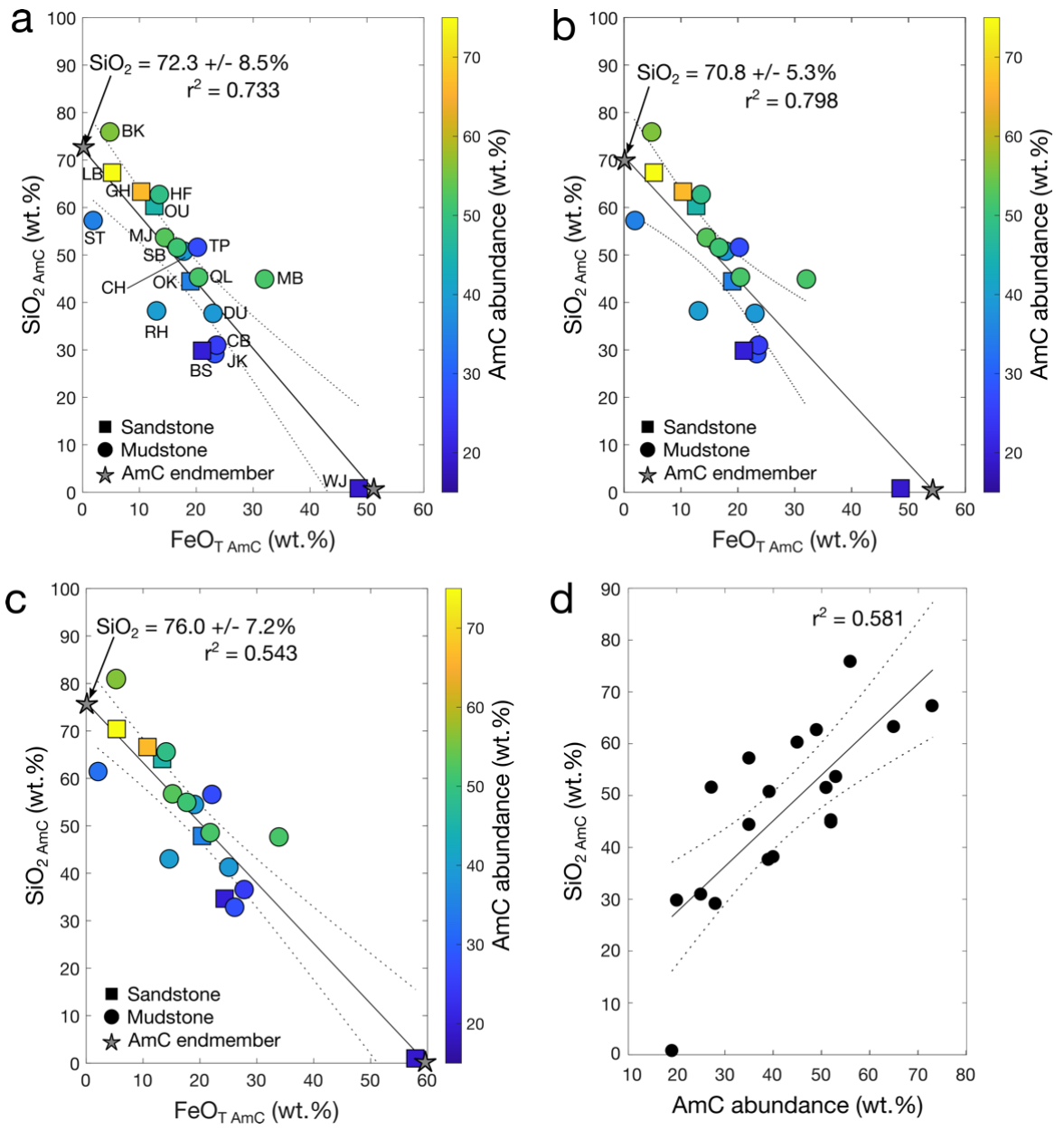

Figure 2. (**a-c**) SiO_2 vs. FeO_T wt% in AmC for drill hole sites listed in Figure 1. Colors represent AmC abundance used in the mass balance calculation (wt%), and symbols represent lithology shown in Figure 1. Solid lines represent the regression and dotted lines ± 2-standard error, interpreted as an approximation to a silica mixing line between FeO_T- and SiO_2-rich endmembers (stars). The y-intercept provides a minimum estimate of the SiO_2 content of the SiO_2-rich endmember. (**a**) Regression performed using the best estimate AmC compositions, and minor elements are included in the AmC composition. (**b**) Regression performed using the same data as in (**a**), but the WJ sample is ignored. (**c**) Regression performed using the best estimate AmC composition, but minor elements have been subtracted from the AmC (see text). (**d**) SiO_2 wt% in AmC vs. AmC abundance (wt%) for all drill hole sites. Solid line represents the regression and dotted lines ± 2-standard error.

(wt% oxide in AmC) of drill hole sites. The Bradbury group rocks sampled by CheMin all have relatively low AmC abundances (between ~17 and 23 wt%), low AmC SiO_2 (~1-30 wt%), and high AmC FeO_T (~23-51 wt%) compared to most overlying sedimentary rocks. However, the Kimberley formation location (WJ) has much lower AmC SiO_2 and much higher AmC FeO_T contents than the Yellowknife Bay formation sedimentary rocks (CB and JK), consistent with the results of Dehouck et al. (2017).

Although the number of Bradbury group samples is limited, there appears to be a noticeable change in AmC properties across the Bradbury-Mount Sharp group transition as the younger, mostly lacustrine Mount Sharp group rocks sampled by CheMin all have moderate to high AmC abundances (between ~27 and 53 wt%), high AmC SiO_2 (~40-75 wt%), and low to

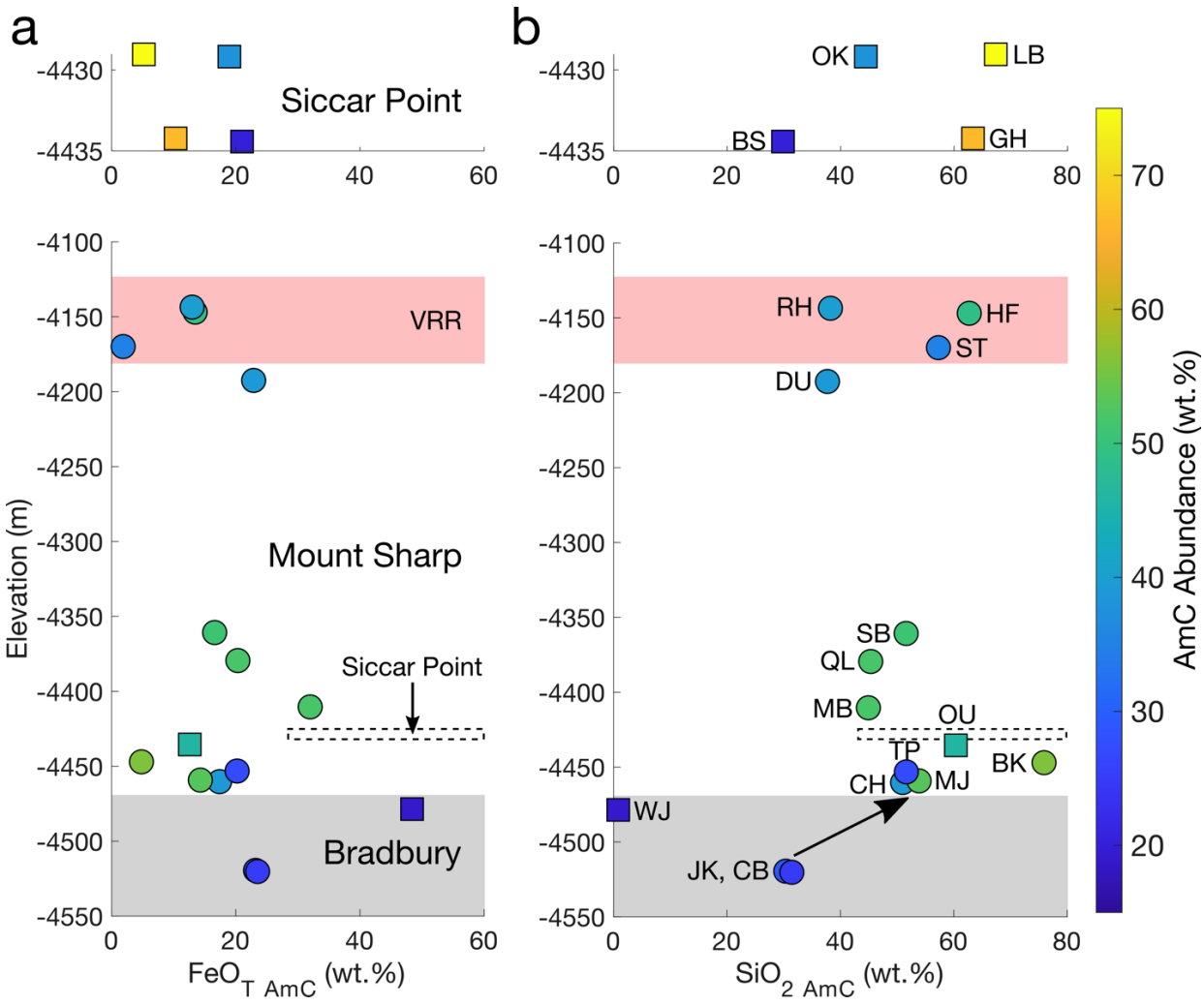

Figure 3. Plots showing stratigraphic variations in AmC FeO_T (**a**) and SiO_2 (**b**) contents (wt%). Siccar Point group data are shown in expanded plots at the top. Symbol colors represent AmC abundances (wt%), and symbol shapes represent lithology (see Figure 2). Drill hole labels are provided in (b). Arrow in (**b**) points to the general increase in AmC SiO_2 content across the Bradbury – Mount Sharp group boundary.

moderate AmC FeO_T (~5-24 wt%). Yet, there is some variation among the Mount Sharp group rocks with anomalous (relative to the drill hole locations stratigraphically above and below) AmC SiO_2 contents at BK, OU, and sedimentary rocks at VRR.

The youngest and unconformably overlying eolian-deposited Siccar Point group rocks analyzed by CheMin have significantly variable AmC properties due to the occurrence of the fracture-associated halos. The parent sedimentary rocks (represented by samples OK and BS) have low AmC abundances (15-20 wt%), relatively low to moderate AmC SiO_2 (~30-45 wt%), and moderate AmC FeO_T (~19-22 wt%). In contrast, the fracture-associated halo drill sites (GH and LB) have the highest AmC abundances of all sedimentary rocks examined (65-73 wt%), high AmC SiO_2 (~64-67 wt%), and low AmC FeO_T (~5-10 wt%).

5 Discussion

5.1 Fire or water?

X-ray amorphous materials may form through volcanic eruptions, impacts, anhydrous oxidative weathering, aqueous chemical weathering and alteration, and direct precipitation from aqueous solutions either as a primary sedimentary deposit or a diagenetic constituent, all of which are possible for the Martian surface, and all of which require water except perhaps for volcanic eruptions, impacts, and anhydrous oxidative alteration. We come to the conclusion that aqueous processes were responsible for most of the variations in AmC SiO_2 and FeO_T in Gale crater sedimentary rocks based on the following observations and supporting arguments.

First, the mixing line in Figure 2 suggests that all rocks in Gale crater contain a few wt% (ST) to ~20 wt% (WJ) of the hypothetical FeO_T-rich AmC endmember (e.g., the WJ rock contains 20 wt% AmC that is ~100% FeO_T-rich endmember). Rocks with the lowest AmC abundances (WJ, JK, CB, BS) have the highest fractions of the FeO_T-rich AmC endmember, and their AmC compositions (~20-50 wt% FeO_T, ~1-30 wt% SiO_2, and other elements related to amorphous material and mass balance calculation artifacts) are not consistent with volcanic or impact glass alone because they would point to an implausibly exotic chemical composition (Dehouck et al., 2014). It is unlikely that anhydrous oxidative weathering products are significantly contributing to the observed AmC because such processes in terrestrial analog environments are only surficial in nature and produce minimal amounts of amorphous materials, primarily oxidizing crystalline phases (Salvatore et al., 2013, 2019).This indicates that the FeO_T-rich AmCs largely formed through aqueous processes involving the alteration of primary minerals and/or glass to precipitate the amorphous (mostly) iron- and silica-bearing material.

Second, the mixing line in Figure 2, along with the observation that AmC abundance increases with AmC SiO_2 suggests that silica-rich AmC material was added to the FeO_T-rich AmC material at some locations (discussed below). The estimated silica content of this silica-rich material could be anywhere in a range from ~64 to 83 wt% SiO_2, which would require dacitic to rhyolitic composition volcanic and impact glasses. Apart from the Buckskin mudstone sample, which contains tridymite and cristobalite (but not quartz) and so may have a felsic volcanic provenance component (Morris et al., 2016), and the Windjana sample, which has been shown to have a mostly trachyte sediment source (Treiman et al., 2016), bulk rock compositions and crystalline component geochemistry and mineralogy provide no evidence for such evolved

compositions contributing to the Gale crater sedimentary rocks studied to date. Therefore, the high-silica AmC endmember also likely resulted from aqueous processes.

Third, mass balance modeling used to constrain the upper limit of glass contribution to the AmCs, shows that each AmC could be comprised of between as much as 0.1 and 57 wt% (median = 10 wt%; average = 17 wt%) basaltic glass of average Martian crust composition (Taylor & McLennan, 2009) (Table S8), leaving behind significant amorphous silica and iron that are not associated with volcanic or impact glass. The maximum fraction of glass was constrained by determining the limiting oxide for each sample, where a greater glass fraction would result in that oxide being left at negative abundance in the remaining amorphous component. For most AmCs, the limiting oxide was Al_2O_3, but in some cases was MgO or CaO, and in one sample each, FeO_T and SiO_2 (Table S8). Note that basaltic glass can have highly variable compositions, and so glasses with lower Al_2O_3 (or whichever the limiting oxide) would increase the possible upper limit of glass, and glasses with higher Al_2O_3 (or whichever the limiting oxide) would decrease the possible upper limit of glass.

5.2 Possible individual X-ray amorphous phases

The mass balance calculation approach provides only a bulk AmC composition, and so we use our knowledge of terrestrial X-ray amorphous materials and the geologic history of Gale crater to speculate on the possible individual phases that comprise the AmCs. X-ray amorphous FeO_T- and/or SiO_2-bearing materials are common components of terrestrial sediments and sedimentary rocks in the form of weathering products, chemical sediments, and diagenetic cements. All of these types of materials could be present in Gale crater, a sedimentary basin that once contained a number of rivers and lakes that were likely connected by a common ground water table (Grotzinger et al., 2015), and experienced diagenetic fluid interactions as recent as 2.12 ± 0.36 Ga based on K-Ar dating of likely diagenetic phases (mostly jarosite) in the Mount Sharp group (Martin et al., 2017).

Just like secondary minerals, the compositions and structures of X-ray amorphous materials formed through aqueous processes depend on fluid compositions, climate, and environmental conditions (Eh, pH, temperature). Iron- and silica-bearing fluids would not be difficult to form on Mars, with a mostly basaltic surface composition enriched in Fe compared the Earth's crust (Taylor and McLennan, 2008). More silica and iron are released during the early stages of aqueous alteration of mafic minerals (e.g., olivine and pyroxene) than felsic minerals (e.g., feldspars and quartz), and so hydrologic reservoirs (e.g., lakes, ground water) in basaltic terrains on Mars could readily be near silica and iron saturation levels (McLennan, 2003; Hurowitz et al., 2017; Tosca et al., 2018). A change in environmental conditions (pH, Eh, temperature) would control where and when iron and silica precipitate, and would also dictate the types of materials that form.

Iron solubility is more dependent on varying environmental conditions than silica. Circum-neutral to acidic (pH < 6-8) and reducing (low Eh) fluids can maintain relatively high Fe^{2+} concentrations. If the pH of low-Eh Fe^{2+}-bearing fluids increases, relatively insoluble Fe^{2+}-hydroxides can precipitate, and if the Eh of Fe^{2+}-bearing fluids increases, Fe^{3+}-(hydr)oxide precipitation will occur at all pH > ~1-3, depending on overall composition (e.g., King and McSween, 2005). On the other hand, silica solubility increases steadily with increasing

temperature, and even more dramatically when pH reaches alkaline conditions (pH > ~9), so solutions could become significantly enriched in silica under alkaline conditions. In fact, basalt dissolution drives the pH of solutions toward more alkaline values (up to pH 10) due to proton consumption by mafic mineral constituents (e.g., Arnórsson et al., 2002). Periodic decreases in silica solubility could be caused by: a decrease in fluid pH through mixing with circum-neutral pH water, atmospheric CO_2, or external acid sources; an increase in ionic strength with the concentration of ground waters (Siever, 1959); and/or temperature fluctuations. Any of these factors could cause silica to become supersaturated and force precipitation, and so fluid pH, temperature, or composition cannot be constrained by silica alone.

The FeO_T-rich AmC material present in all Gale crater rocks does not necessarily represent a single composition precipitated by a single process, but likely represents compositionally variable assemblages consisting of several amorphous materials. Suboxic conditions might have formed $Fe^{2+/3+}$-materials co-precipitated with silica, possibly green rust (Tosca et al., 2018). On the other hand, oxidizing conditions might have formed Fe^{3+}-materials such as hisingerite ($Fe_2O_3 \cdot SiO_2 \cdot 2H_2O$) or silica + ferrihydrite ($5Fe_2O_3 \cdot 9H_2O$) (Dehouck et al., 2014, 2017), similar to nanophase Fe^{3+}-oxides detected in rocks and soils at Gusev crater and Meridiani Planum by the Mössbauer spectrometers onboard the *Spirit* and *Opportunity* rovers (Morris et al., 2006) and inferred in some Gale crater rocks from Mastcam spectra (Horgan et al., 2020). Poorly crystalline nontronite, Fe-sulfates (Sutter et al., 2017; Achilles et al., 2020), amorphous Fe-phosphate (Tu et al., 2014), anhydrous oxidative weathering products (Salvatore et al., 2013, 2019), and minor glass are also potential contributors to the FeO_T-rich AmC material.

The estimated composition of the SiO_2-rich AmC endmember is not pure silica, but could represent opaline silica intimately mixed with other phases, or cation-bearing X-ray amorphous silicates. Opaline silica forms in soils during pedogenesis (e.g., Chadwick et al., 1987; Drees et al., 1989), as chemical sediments on sea floors (e.g., Iijima and Tada, 1981), as precipitates from groundwater at springs and in sediments (e.g., Channing and Butler, 2007; Rodgers et al., 2003; Martin and Gaillou, 2018), and it is a cementing agent for many types of sedimentary rocks (Scholle and Ulmer-Scholle, 2003). In such natural environments, amorphous silica can co-precipitate with other materials. For instance, nanoparticles of amorphous iron and silica formed by chemical precipitation from the water column are thought to be the precursors for Precambrian banded iron formation rocks (e.g., Rasmussen et al., 2015). The "impurity" of the silica endmember could also be explained by (Mg^{2+}, $Fe^{2+/3+}$, Ca^{2+}, Na^{+}, K^{+})-bearing X-ray amorphous silicates, such as those that have been shown to form during chemical weathering and alteration in cold climate mafic terrains (e.g., Rutledge et al., 2018; Thorpe et al., 2019; Smith et al., 2017). Amorphous silica-rich deposits have been detected across the Martian surface by both orbiter and rover-based instruments (e.g., Bandfield, 2002; Squyres et al., 2008; Milliken et al., 2008; Fraeman et al., 2016; Sun and Milliken, 2018; Tarnas et al., 2019), and in Martian meteorites using terrestrial laboratory techniques (e.g., Lee et al., 2015). The finding of an

amorphous silica-rich endmember throughout rocks drilled from Gale crater reinforces the importance of amorphous silica-forming processes throughout the history of the planet.

5.3 Constraining processes and timing in Gale crater

It is important to emphasize that AmC compositions could represent complex combinations of materials formed through different processes at different times. Sedimentary basins on Earth are reservoirs for detrital and authigenic sediments, with regional and local ground water circulation patterns and environmental conditions that vary significantly in space and time (e.g., Morad et al., 2000). All of these factors determine what phases are present at any given location or time. We see evidence for such variations within Gale crater as there are variable ratios of likely authigenic and/or diagenetic redox sensitive Fe-bearing minerals (magnetite and hematite), indicating variable Eh conditions within stratigraphic groups (Hurowitz et al., 2017; Rampe et al., 2020a and references therein). Additionally, later diagenetic fluids could overprint detrital or earlier diagenetic deposits.

We separate possible formation processes for Gale crater amorphous SiO_2- and FeO_T-bearing materials into three time frames: (1) pre-deposition of sediments (i.e., provenance and chemical weathering history in the sediment source region), (2) syn-deposition to early post-deposition of sediments (i.e., authigenic to early diagenetic), and (3) post-deposition of sediments (i.e., mid to late diagenetic) (Figure 4). X-ray amorphous materials formed in the pre-deposition time frame would have formed in the source region before being transported to the crater (i.e., detrital; Figure 4, top). As such, these materials would indicate processes happening in the source regions around the late Noachian epoch (Thomson et al., 2011), a time period over which there is continuing debate about if the climate was warm and wet, cold and icy, or somewhat variable at any given time (e.g., Wordsworth, 2016; Ramirez and Craddock, 2018; McLennan et al., 2019). Authigenic amorphous materials formed during the syn-depositional to early post-depositional time frame would be indicative of physicochemical conditions in the lakes and sediment pore spaces (connate fluids) around the time of deposition (Figure 4, middle). Precipitation of chemical precipitates from the water column would allow for chemical sediments to build up along with the detrital siliciclastic sediments (syndepositional). Shortly following deposition on the crater floor, and with increased burial, water trapped in the sediment pore spaces might precipitate cements (e.g., Siever, 1959; Pettijohn et al., 1987). Post-lithification (i.e., mid to late diagenesis), authigenic X-ray amorphous materials could also have formed from interactions with locally or regionally sourced diagenetic fluids circulating through the rocks (Figure 4, bottom). This later time period is typically characterized by much more extensive cementation during moderate burial (mid diagenesis; e.g., Siever, 1959; Pettijohn et al., 1987), and alteration reactions (late diagenesis; e.g., Morad et al., 2000).

Pre-deposition of sediments (detrital)

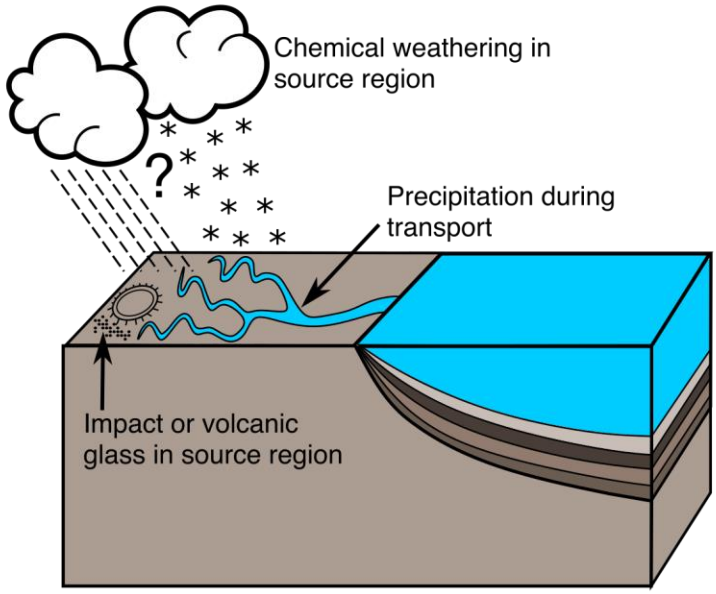

Syn-depositional to early diagenesis (authigenic)

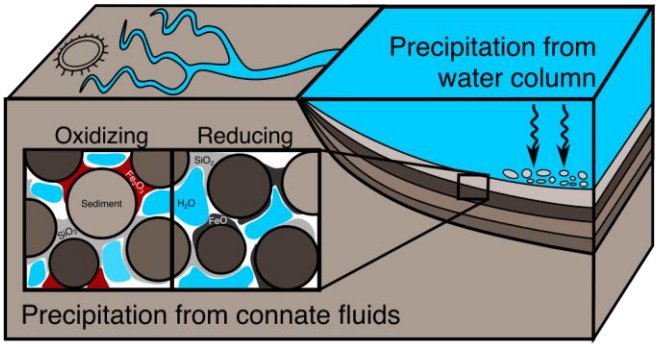

Post-deposition of sediments (authigenic)

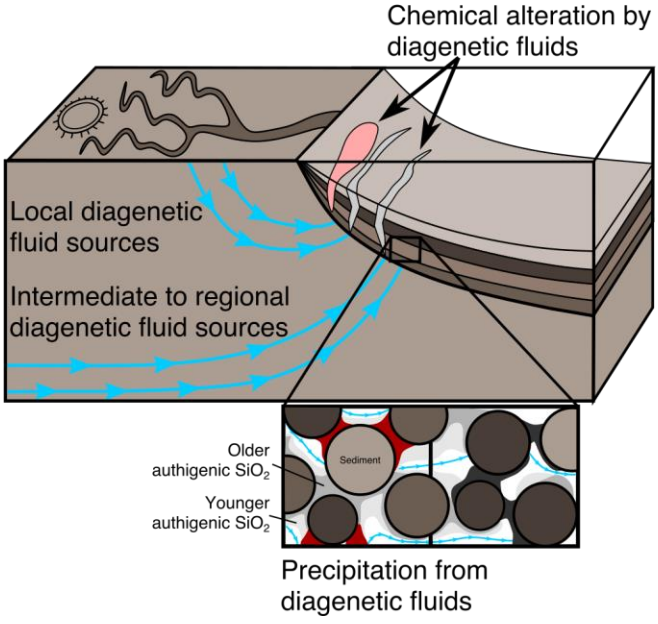

Figure 4. Illustrations showing the relative timing of the potential processes forming the amorphous SiO_2 and FeO_T components of sedimentary rocks in Gale crater. (**Top**) Detrital amorphous materials could have formed through volcanic eruptions or impacts (glass), chemical weathering in the source region, or during fluvial transport before being deposited in Gale crater. (**Middle**) Authigenic amorphous materials could have formed during sediment deposition by precipitation from the water column as chemical sediments or from connate fluids as pore space cement after sediment deposition. (**Bottom**) Authigenic amorphous materials could have formed after sediment deposition by precipitation from diagenetic fluids in remaining pore spaces or by chemical alteration of the lithified rock with diagenetic fluids.

Crosscutting relationships and geologic context provide evidence that some of the AmCs are related to late diagenetic processes. Two of the most SiO_2-rich AmCs are found in alteration halos (GH and LB) associated with fractures that crosscut the Siccar Point group parent rocks, indicating that the alteration took place sometime after the rocks were lithified and fractured (Frydenvang et al., 2017; Yen et al., 2017; Hausrath et al., 2018). This crosscutting relationship also indicates that the compositionally distinct AmCs in the parent rocks were formed earlier (pre-deposition to mid diagenesis time frames).

Late diagenetic AmC SiO_2-enrichment may not have been limited to the Siccar Point group rocks. Gabriel et al. (2019) reported on a large fracture network in the Bradbury group that shows similar surface expression, geochemical trends, and estimated water content compared to the fracture-associated halos in the Siccar Point group. Additionally, while not associated with fractures, the Buckskin (BK), Oudam (OU), Stoer (ST), and Highfield (HF) drill hole locations in the Mount Sharp group have AmCs that are very enriched in SiO_2 compared to the drill hole locations stratigraphically above and below, suggesting localized fluid interactions (e.g., Morris et al., 2016; Achilles et al., 2020; Yen et al., 2020). Fluids migrating through localized zones in the rocks could have either provided a new silica source (e.g., Frydenvang et al., 2017) or allowed for the passive enrichment of silica by leaching (e.g., Yen et al., 2017) or by crystallizing amorphous iron oxides (e.g., Achilles et al., 2020; discussed below). Accordingly, the most SiO_2-rich AmCs observed in Gale crater thus far may result from fluid interactions long after the lithification of the parent sedimentary rocks. The fact that these observations occur across the rover traverse suggest that localized fluids were widespread throughout Gale crater, possibly over long periods of time, at least until after the youngest sedimentary rocks had been lithified.

Not all amorphous SiO_2 enrichment resulted from localized late diagenetic fluids. The broad increase in AmC abundance and SiO_2 content across the Bradbury – Mount Sharp boundary coincides with differences in provenance (Siebach et al., 2017; Bedford et al., 2018) and an observed increase in bulk rock SiO_2 (Hurowitz et al., 2017). Hurowitz et al. (2017) hypothesized that increased bulk rock SiO_2 was evidence for amplified source region chemical weathering due to wetter climate conditions during deposition of the Mount Sharp group, and bulk rock chemical analyses provide further evidence that Mount Sharp group rocks are more intensely weathered (e.g., Siebach et al., 2017; Mangold et al., 2019). Increased weathering could have supplied detrital X-ray amorphous (Mg^{2+}, $Fe^{2+/3+}$)-rich silicates along with the crystalline detrital sediments (Figure 4, top), and SiO_2-bearing, alkaline surface- and ground-waters to Gale crater (Figure 4, middle and bottom). Decreases in pH by mixing with circum-neutral waters, or even local evaporation could have allowed for silica supersaturation, possibly

leading to precipitation from the water column or in pore spaces as cements. Thus, the overall enrichment in amorphous silica for the Mount Sharp group rocks, relative to the Bradbury group rocks, is likely due to processes in the pre-depositional through mid-diagenesis time frames, with additional amorphous silica enrichment in some locations resulting from late diagenetic overprinting (BK, OU, ST, and HF, as discussed above).

5.4 The problem with preservation

It is not necessarily difficult to form X-ray amorphous materials on Mars, and in theory it would not be difficult to accumulate them in a sedimentary basin such as Gale crater, a terminal sink for materials formed through a variety of processes. But their preservation for up to billions of years is a major conundrum for understanding the Martian sedimentary rock cycle (McLennan et al., 2019). X-ray amorphous materials are metastable and are thought to recrystallize on very short timescales (e.g., Curtis, 1977, 1990; Siever, 1983; Tosca and Knoll, 2009). Crystallization processes such as Ostwald ripening (Steefel and Van Cappellen, 1990) and crystallization through particle attachment (De Yoreo et al., 2015) result from prolonged aqueous interactions which drive dissolution/reprecipitation processes that allow atomic and particle rearrangements to take place. Thus, more crystalline alteration products are formed at the expense of amorphous materials through particle coarsening processes determined by both kinetic and thermodynamic factors. As a result, X-ray amorphous materials have yet to be found in significant abundances in rocks of comparable age (> 1 Gy) on Earth. Indeed, on Earth X-ray amorphous materials of greater than ~10 My in age are exceedingly rare in sedimentary rocks.

Based on the crystalline mineralogy at each drill hole location, there is some indication that portions of the AmC materials might have been converted to more crystalline materials during diagenesis. For instance, opal-CT is detected in the Oudam (OU) drill hole sample, which may represent the diagenesis of opal-A (Achilles et al., 2020). Another example is the Stoer (ST) drill hole sample, which has an anomalous AmC composition compared to other drill hole locations with moderate AmC abundances. The FeO_T-poor, SiO_2-rich AmC of Stoer coupled with the highest hematite abundances detected at VRR (Rampe et al., 2020b) could be evidence for the crystallization of hematite from originally amorphous FeO_T during diagenetic fluid interactions. Despite the fact that some fraction of the AmC materials might have been converted to more crystalline alteration products, all of these sedimentary rocks contain significant abundances of X-ray amorphous materials that have been preserved for billions of years.

Orbital detections of hydrated amorphous silica (and other poorly crystalline minerals) in ancient deposits across the Martian surface led Tosca and Knoll (2009) to conclude that the preservation of such phases indicated a water-limited environment since they formed. However, our understanding of Martian aqueous history has changed significantly with the study of Gale crater by the *Curiosity* rover (see review in McLennan et al., 2019). Along with the results from this study, there is substantial evidence for a long history of water-rock interactions in Gale crater (e.g., Léveillé et al., 2014; Stack et al., 2014; Nachon et al., 2014, 2017; Frydenvang et al., 2017; Kah et al., 2018; Minitti et al., 2019; Sun et al., 2019). In fact, likely diagenetic jarosite in the Mount Sharp group sample MJ has a K-Ar age date <3 Ga and possibly as young as ~2.1 Ga, showing that diagenetic fluids circulated through the buried sediments for up to a billion years or more post emplacement (Martin et al., 2017). A long history of liquid water in Gale crater, however, does not necessarily mean that liquid water was continuously present for billions of

years. Perhaps shorter durations of water-rock interactions might have allowed amorphous materials to form but not transform to crystalline products. Nevertheless, given our current knowledge about the instability of X-ray amorphous materials, it continues to remain unclear how the X-ray amorphous materials in Gale crater have been preserved nearly intact through to the present-day.

6 Conclusions and Outstanding Questions

AmC SiO_2 and FeO_T contents are anti-correlated suggesting a mixing relationship between hypothetical SiO_2-rich and FeO_T-rich AmC endmembers. The compositions of the hypothetical endmembers are inconsistent with volcanic or impact glass alone, and so we conclude that the SiO_2 and FeO_T contents in the X-ray amorphous material in Gale crater sedimentary rocks formed largely through aqueous processes.

The individual constituents of the AmCs likely formed through aqueous processes occurring both outside and inside the crater at different times, such that the bulk AmCs represent mixtures of individual X-ray amorphous materials (e.g., weathering products, chemical sediments, and diagenetic cements) accumulated over time. The FeO_T-rich AmC materials likely comprise mixtures of Fe-silicates, ferrous or ferric oxide nanoparticles, SiO_2, Fe-sulfates, various non-Fe-bearing amorphous materials, and minor glass. The hypothetical SiO_2-rich endmember is not pure opaline silica, but could represent opaline silica co-precipitated with other phases (e.g., sulfates) or cation-rich silicates.

The AmC SiO_2 and FeO_T contents in Gale crater rocks represent materials mostly formed through long-lived aqueous processes that started before the first sediments were deposited in the crater (late Noachian), and did not end until well after the youngest sediments were lithified (mid Hesperian, possibly late Hesperian). Cross-cutting relationships and geologic context provide evidence that the most SiO_2-rich AmCs observed in Gale crater thus far may result from localized fluids having either provided a new silica source or passively enriched the rocks in silica long after the lithification of the parent sedimentary rocks. On the other hand, AmCs with moderate to low SiO_2 contents likely formed much earlier in the pre-depositional through mid diagenetic time frames.

Two fundamental problems remain in understanding the amorphous components of Martian sedimentary rocks. The first is why is there so much amorphous material of such variable composition in Martian sedimentary rocks, and the second is how are these materials preserved over billions of years? Perhaps at a fundamental level these questions are related. The basic mechanisms identified for the formation of possible amorphous components in Martian sedimentary rocks are individually well-documented and well-understood from the terrestrial sedimentary rock record: igneous and impact glasses, chemical weathering products, chemical sedimentation, precipitation of syn-depositional through late stage diagenetic phases (e.g., Curtis, 1977; Pettijohn et al., 1987). However, on Earth, these phases are thermodynamically unstable and recrystallize on very short timescales (e.g., Curtis, 1977, 1990; Siever, 1983; Tosca and Knoll, 2009; also see De Yoreo et al., 2015). Accordingly, amorphous materials formed by different processes are less likely to accumulate throughout the source-to-sink history of a sedimentary rock, and where they are more likely to accumulate (e.g., chemical and fine-grained clastic sedimentary rocks) they do not persist long after burial (Curtis, 1990). On Mars, the

situation appears to be different in that there must be long-lived (>10^9 yr), but poorly understood, kinetic, or perhaps even thermodynamic (e.g., persistent metastability; De Yoreo et al., 2015), impediments to the recrystallization of amorphous materials. In addition, the basaltic nature of the eroding Martian crust is likely to be more efficient in forming amorphous materials, especially during early stages of chemical weathering, than is the granitic upper continental crust of the Earth (e.g., McLennan, 2003). Thus, for Martian sedimentary rocks, perhaps it should not be unexpected that amorphous materials, derived from a variety of sources and processes, accumulate in sedimentary rocks throughout the source-to-sink history and diagenesis. Such a history would lead to both relatively high abundances of amorphous materials and to a diversity of amorphous phases compared to what is typically seen in the terrestrial sedimentary record. Nevertheless, although post-depositional aqueous history is likely to be a factor, the reasons for the exceptional persistence of such materials in the Martian geological record remains largely an open question.

Acknowledgments, Samples, and Data

There are no real or perceived financial conflicts of interests for any author. All data supporting the conclusions can be obtained within the article and in the referenced published work, or in the Supplemental Material (Smith R., 2021) found here: http://dx.doi.org/10.17632/srm3v7sr76.3. This work was funded through a NASA Participating Scientist award to SMM (JPL Subcontract 1457128). A portion of this research was carried out at the Jet Propulsion Laboratory, California Institute of Technology, under a contract with the National Aeronautics and Space Administration (80NM0018D0004). We thank Shaunna Morrison for providing assistance with CheMin interpretations, Troy Rasbury for assistance with statistics, and Linda Kah, Steven Chemtob, and one anonymous reviewer for providing helpful comments that greatly improved a previous version of this manuscript.

References

Achilles, C. N., Downs, R. T., Ming, D. W., Rampe, E. B., Morris, R. V., Treiman, A. H., et al. (2017). Mineralogy of an active eolian sediment from the Namib dune, Gale crater, Mars. *Journal of Geophysical Research: Planets*, 122(11), 2344-2361. doi: 10.1002/2017je005262

Achilles, C.N., Rampe, E.B., Downs, R.T., Bristow, T.F., Ming, D.W., Morris, R.V., et al. (2020). Evidence for Multiple Diagenetic Episodes in Ancient Fluvial-Lacustrine Sedimentary Rocks in Gale Crater, Mars. *Journal of Geophysical Research: Planets*, 125(8). https://doi.org/10.1029/2019JE006295

Arnórsson, S., I. Gunnarsson, A. Stefánsson, A. Andrésdóttir, & Á. E. Sveinbjörnsdóttir (2002). Major element chemistry of surface- and ground waters in basaltic terrain, N-Iceland. *Geochimica et Cosmochimica Acta*, 66(23), 4015-4046. doi: 10.1016/s0016-7037(02)00991-2

Badaut, D., Decarreau, A., & Besson, G. (1992). Ferripyrophyllite and related Fe^{3+}-rich 2:1 clays in Recent deposits of Atlantis II Deep, Red Sea. *Clay Minerals*, 27(2), 227-244. doi: 10.1180/claymin.1992.027.2.07

Bandfield, J. L. (2002). Global mineral distributions on Mars. *Journal of Geophysical Research*, 107(E6). doi: 10.1029/2001je001510

Banham, S. G., Gupta, S., Rubin, D. M., Watkins, J. A., Sumner, D. Y., Edgett, K. S., et al. (2018). Ancient Martian aeolian processes and palaeomorphology reconstructed from the Stimson formation on the lower slope of Aeolis Mons, Gale crater, Mars. *Sedimentology*, 65(4), 993-1042. doi: 10.1111/sed.12469

Bedford, C. C., Bridges, J. C., Schwenzer, S. P., Wiens, R. C., Rampe, E. B., Frydenvang, J., & Gasda, P. J. (2018). Alteration trends and geochemical source region characteristics preserved in the fluviolacustrine sedimentary record of Gale crater, Mars. *Geochimica Et Cosmochimica Acta*, 246, 234-266. doi: 10.1016/j.gca.2018.11.031

Bedford, C. C., Schwenzer, S. P., Bridges, J. C., Banham, S., Wiens, R. C., Gasnault, O., et al. (2020). Geochemical variation in the Stimson formation of Gale crater: Provenance, mineral sorting, and a comparison with modern Martian dunes. *Icarus*, 341, 113622. doi: 10.1016/j.icarus.2020.113622

Berger, J. A., Gellert, R., Boyd, N. I., King, P. L., McCraig, M. A., O'Connell-Cooper, C. D., et al. (2020). Elemental composition and chemical evolution of geologic materials in Gale crater, Mars: APXS results from Bradbury Landing to the Vera Rubin Ridge. *Journal of Geophysical Research: Planets*. doi: https://doi.org/10.1029/2020JE006536

Blake, D., Vaniman, D., Achilles, C., Anderson, R., Bish, D., Bristow, T., et al. (2012). Characterization and Calibration of the CheMin Mineralogical Instrument on Mars Science Laboratory. *Space Science Reviews*, 170(1-4), 341-399. doi: 10.1007/s11214-012-9905-1

Blake, D. F., Morris, R. V., Kocurek, G., Morrison, S. M., Downs, R. T., Bish, D., et al. (2013). Curiosity at Gale crater, Mars: Characterization and analysis of the Rocknest sand shadow. *Science*, 341(6153), 1239505. doi: 10.1126/science.1239505

Blaney, D. L., Wiens, R. C., Maurice, S., Clegg, S. M., Anderson, R. B., Kah, L. C., et al. (2014). Chemistry and texture of the rocks at Rocknest, Gale Crater: Evidence for sedimentary origin and diagenetic alteration. *Journal of Geophysical Research: Planets*, 119(9), 2109-2131. doi: 10.1002/2013je004590

Brigatti, M. F. (1983). Relationships between Composition and Structure in Fe-Rich Smectites. *Clay Minerals*, 18(2), 177-186. doi: 10.1180/claymin.1983.018.2.06

Bristow, T. F., Bish, D. L., Vaniman, D. T., Morris, R. V., Blake, D. F., Grotzinger, J. P., et al. (2015). The origin and implications of clay minerals from Yellowknife Bay, Gale crater, Mars. *American Mineralogist*, 100(4), 824-836. doi: 10.2138/am-2015-5077CCBYNCND

Bristow, T. F., Rampe, E. B., Achilles, C. N., Blake, D. F., Chipera, S. J., Craig, P., et al. (2018). Clay mineral diversity and abundance in sedimentary rocks of Gale crater, Mars. *Science Advances*, 4(6), eaar3330. doi: 10.1126/sciadv.aar3330

Chadwick, O. A., Hendricks, D. M., & Nettleton, W. D. (1987). Silica in Duric Soils: II. Mineralogy. *Soil Science Society of America Journal*, 51(4), 982-985. doi: 10.2136/sssaj1987.03615995005100040029x

Channing, A., & Butler, I. B. (2007). Cryogenic opal-A deposition from Yellowstone hot springs. *Earth and Planetary Science Letters*, 257(1-2), 121-131. doi: 10.1016/j.epsl.2007.02.026

637 Curtis, C. D. (1977). Sedimentary geochemistry: Environments and processes dominated by
638 involvement of an aqueous phase. *Philosophical Transactions of the Royal Society of*
639 *London.* Series A, Mathematical and Physical Sciences, 286(1336), 353-372.

640 Curtis, C. D. (1990). Aspects of climatic influence on the clay mineralogy and geochemistry of
641 soils, paleosols and clastic sedimentary rocks. *Journal of the Geological Society of*
642 *London*, 147(2), 351-357.

643 David, G., Cousin, A., Forni, O., Meslin, P.-Y., Dehouck, E., Mangold, N., et al.
644 (2020). Analyses of high-iron sedimentary bedrock and diagenetic features observed with
645 ChemCam at Vera Rubin Ridge, Gale Crater, Mars: Calibration and
646 characterization. *Journal of Geophysical Research: Planets*, 125,
647 e2019JE006314. https://doi.org/10.1029/2019JE006314

648 Day, M., Anderson, W., Kocurek, G., & Mohrig, D. (2016). Carving intracrater layered deposits
649 with wind on Mars. *Geophysical Research Letters*, 43(6), 2473-2479. doi:
650 10.1002/2016gl068011

651 De Yoreo, J. J., Gilbert, P. U. P. A., Sommerdijk, N. A. J. M., Penn, R. L., Whitelam, S., Joester,
652 D., et al. (2015). Crystallization by particle attachment in synthetic, biogenic, and
653 geologic environments. *Science*, 349(6247), aaa6760-aaa6760. doi:
654 10.1126/science.aaa6760

655 Dehouck, E., McLennan, S. M., Meslin, P.-Y., & Cousin, A. (2014). Constraints on abundance,
656 composition, and nature of X-ray amorphous components of soils and rocks at Gale
657 crater, Mars. *Journal of Geophysical Research: Planets*, 119(12), 2640-2657. doi:
658 10.1002/2014je004716

659 Dehouck, E., McLennan, S. M., Sklute, E. C., and Dyar, M. D. (2017). Stability and fate of
660 ferrihydrite during episodes of water/rock interactions on early Mars: An experimental
661 approach. *Journal of Geophysical Research: Planets*, 122(2), 358-382. doi:
662 10.1002/2016je005222

663 Drees, L. R., Wilding, L. P., Smeck, N. E. and Senkayi, A. L. (2018). Silica in Soils: Quartz and
664 Disordered Silica Polymorphs. In J.B. Dixon and S.B. Weed (Eds.), *Minerals in Soil*
665 *Environments*, Soil Science Society of America series. doi:10.2136/sssabookser1.2ed.c19

666 Edgar, L. A., Gupta, S., Rubin, D. M., Lewis, K. W., Kocurek, G. A., Anderson, R. B., et al.
667 (2017). Shaler: in situ analysis of a fluvial sedimentary deposit on Mars. *Sedimentology*,
668 65(1), 96-122. doi: 10.1111/sed.12370

669 Edwards, P. H., Bridges, J. C., Wiens, R., Anderson, R., Dyar, D. Fisk, M., et al. (2017). Basalt-
670 trachybasalt samples in Gale Crater, Mars. *Meteoritics & Planetary Science*. doi:
671 10.1111/maps.12953

672 Fraeman, A. A., Edgar, L. A., Rampe, E. B., Thompson, L. M., Frydenvang, J., Fedo, C. M., et
673 al. (2020). Evidence for a Diagenetic Origin of Vera Rubin Ridge, Gale Crater, Mars:
674 Summary and Synthesis of Curiosity's Exploration Campaign. *Journal of Geophysical*
675 *Research: Planets*. doi: 10.1029/2020je006527

676 Fraeman, A. A., Ehlmann, B. L., Arvidson, R. E., Edwards, C. S., Grotzinger, J. P., Milliken, R.
677 E., et al. (2016). The stratigraphy and evolution of lower Mount Sharp from spectral,

morphological, and thermophysical orbital data sets. *Journal of Geophysical Research: Planets*, 121(9), 1713-1736. doi: 10.1002/2016JE005095

Frydenvang, J., Gasda, P. J., Hurowitz, J. A., Grotzinger, J. P., Wiens, R. C., Newsom, H. E., et al. (2017). Diagenetic silica enrichment and late-stage groundwater activity in Gale crater, Mars. *Geophysical Research Letters*, 44(10), 4716-4724. doi: 10.1002/2017gl073323

Gabriel, T. S. J., Hardgrove, C., Achilles, C., Rampe, E. B., Czarnecki, S., Rapin, W., et al. (2019). Pervasive water-rich, fracture-associated alteration halos in Gale crater, Mars. Paper presented at the American Geophysical Union Fall Meeting 2019, San Francisco, CA.

Gellert, R., Clark, B. C., MSL Science Team, & MER Science Team (2015). In Situ Compositional Measurements of Rocks and Soils with the Alpha Particle X-ray Spectrometer on NASA's Mars Rovers. Elements, 11(1), 39-44. doi: 10.2113/gselements.11.1.39

Grant, J. A., S. A. Wilson, N. Mangold, F. Calef, & J. P. Grotzinger (2014). The timing of alluvial activity in Gale crater, Mars. *Geophysical Research Letters*, 41(4), 1142-1149. doi: 10.1002/2013gl058909

Grotzinger, J. P., Gupta, S., Malin, M. C., Rubin, D. M., Schieber, J., Siebach, K., et al. (2015). Deposition, exhumation, and paleoclimate of an ancient lake deposit, Gale crater, Mars. *Science*, 350(6257), aac7575. doi: 10.1126/science.aac7575

Grotzinger, J. P., Sumner, D. Y., Kah, L. C., Stack, K., Gupta, S., Edgar, L., et al. (2014). A Habitable Fluvio-Lacustrine Environment at Yellowknife Bay, Gale Crater, Mars. *Science*, 343(6169). doi: 10.1126/science.1242777

Harsh, J. (2005). Amorphous materials. In D. Hillel (Ed.), *Encyclopedia of Soils in the Environment* (Vol. 3, p. 64), New York, NY: Academic Press.

Hausrath, E. M., Ming, D. W., Peretyazhko, T. S., & Rampe, E. B. (2018). Reactive transport and mass balance modeling of the Stimson sedimentary formation and altered fracture zones constrain diagenetic conditions at Gale crater, Mars. *Earth and Planetary Science Letters*, 491, 1-10.

Horgan, B. H. N., Johnson, J. R., Fraeman, A. A., Rice, M. S., Seeger, C., Bell III, J. F., et al. (2020) Diagenesis of Vera Rubin ridge, Gale crater, Mars from Mastcam multispectral images. *Journal of Geophysical Research: Planets*, 125, e2019JE006322. https://doi.org/10.1029/2019JE006322

Hurowitz, J. A., Grotzinger, J. P., Fischer, W. W., McLennan, S. M., Milliken, R. E., Stein, N., et al. (2017). Redox stratification of an ancient lake in Gale crater, Mars. *Science*, 356(6341). doi: 10.1126/science.aah6849

Iijima, A., & Tada, R. (1981). Silica diagenesis of Neogene diatomaceous and volcaniclastic sediments in northern Japan. *Sedimentology*, 28(2), 185-200. doi: 10.1111/j.1365-3091.1981.tb01676.x

Kah, L. C., Stack, K. M., Eigenbrode, J. L., Yingst, R. A., & Edgett, K. S. (2018). Syndepositional precipitation of calcium sulfate in Gale Crater, Mars. *Terra Nova*, 30(6), 431-439. doi: 10.1111/ter.12359

King, P. L., & McSween, H. Y. (2005). Effects of H_2O, pH, and oxidation state on the stability of Fe minerals on Mars. *Journal of Geophysical Research*, 110(E12). doi: 10.1029/2005je002482

Kronyak, R. E., Kah, L. C., Miklusicak, N. B., Edgett, K. S., Sun, V. Z., Bryk, A. B., & Williams, R. M. E. (2019). Extensive Polygonal Fracture Network in Siccar Point group Strata: Fracture Mechanisms and Implications for Fluid Circulation in Gale Crater, Mars. *Journal of Geophysical Research: Planets*, 124(10), 2613-2634. doi: 10.1029/2019je006125

Le Deit, L., E. Hauber, F. Fueten, M. Pondrelli, A. P. Rossi, & R. Jaumann (2013). Sequence of infilling events in Gale Crater, Mars: Results from morphology, stratigraphy, and mineralogy. *Journal of Geophysical Research: Planets*, 118(12), 2439-2473. doi: 10.1002/2012je004322

Lee, M. R., MacLaren, I., Andersson, S. M. L., Kovács, A., Tomkinson, T., Mark, D. F., & Smith, C. L. (2015). Opal-A in the Nakhla meteorite: A tracer of ephemeral liquid water in the Amazonian crust of Mars. *Meteoritics & Planetary Science*, 50(8), 1362-1377. doi: 10.1111/maps.12471

Leshin, L. A., Mahaffy, P. R., Webster, C. R., Cabane, M., Coll, P., Conrad, P. G., et al. (2013). Volatile, Isotope, and Organic Analysis of Martian Fines with the Mars Curiosity Rover. *Science*, 341(6153), 1238937-1238937. doi: 10.1126/science.1238937

Léveillé, R.J., Bridges, J., Wiens, R.C., Mangold, N., Cousin, A., Lanza, N., et al. (2014). Chemistry of fracture-filling raised ridges in Yellowknife Bay, Gale Crater: Window into past aqueous activity and habitability on Mars. *Journal of Geophysical Research: Planets*, 119(11), 2398-2415. doi: 10.1002/2014je004620

L'Haridon, J., Mangold, N., Fraeman, A. A., Johnson, J. R., Cousin, A., Rapin, W., et al. (2020). Iron Mobility during Diagenesis at Vera Rubin ridge, Gale Crater, Mars. *Journal of Geophysical Research: Planets*, 125, e2019JE006299. https://doi.org/10.1029/2019JE006299

Mack, G.H., James, W.C., & Monger, H.C. (1993). Classification of paleosols. *Bulletin of the Geological Society of America*, 105(2), 129-136.

Malin, M. C., & K. S. Edgett (2000), Sedimentary Rocks of Early Mars, Science, 290(5498), 1927-1937, doi: 10.1126/science.290.5498.1927.

Mangold, N., Dehouck, E., Fedo, C., Forni, O., Achilles, C., Bristow, T., et al. (2019). Chemical alteration of fine-grained sedimentary rocks at Gale crater. *Icarus*, 321, 619-631. doi: 10.1016/j.icarus.2018.11.004

Martin, E., & Gaillou, E. (2018). Insight on gem opal formation in volcanic ash deposits from a supereruption: A case study through oxygen and hydrogen isotopic composition of opals from Lake Tecopa, California, U.S.A. *American Mineralogist*, 103(5), 803-811. doi: 10.2138/am-2018-6131

Martin, P.E., Farley, K.A., Baker, M.B., Malespin, C.A., Schwenzer, S.P., Cohen, B.A., et al. (2017). A two-step K-Ar experiment on Mars: Dating the diagenetic formation of jarosite from Amazonian groundwaters. *Journal of Geophysical Research: Planets*, 122(12), 2803-2818. doi: 10.1002/2017je005445

McLennan, S. M. (2003). Sedimentary silica on Mars. *Geology*, 31(4), 315-318. doi: 10.1130/0091-7613(2003)031<0315:SSOM>2.0.CO;2

McLennan, S. M., Grotzinger, J. P., Hurowitz, J. A., & Tosca, N. J. (2019). The Sedimentary Cycle on Early Mars. *Annual Review of Earth and Planetary Sciences*, 47(1). doi: 10.1146/annurev-earth-053018-060332

Milliken, R.E., Swayze, G.A., Arvidson, R.E., Bishop, J.L., Clark, R.N., Ehlmann, B.L., et al. (2008). Opaline silica in young deposits on Mars. *Geology*, 36(11). 847-850. doi: 10.1130/G24967A.1

Minitti, M. E., Malin, M. C., Van Beek, J. K., Caplinger, M., Maki, J. N., Ravine, M., et al. (2019). Distribution of primary and secondary features in the Pahrump Hills outcrop (Gale crater, Mars) as seen in a Mars Descent Imager (MARDI) "sidewalk" mosaic. *Icarus*, 328, 194-209. doi: 10.1016/j.icarus.2019.03.005

Morad, S., Ketzer, J. M., & De Ros, L. F. (2000). Spatial and temporal distribution of diagenetic alterations in siliciclastic rocks: Implications for mass transfer in sedimentary basins. *Sedimentology*, 47, 95-120. doi: 10.1046/j.1365-3091.2000.00007.x

Morris, R.V., Klingelhöfer, G., Schröder, C., Rodionov, D.S., Yen, A., Ming, D.W., et al. (2006). Mössbauer mineralogy of rock, soil, and dust at Gusev crater, Mars: Spirit's journey through weakly altered olivine basalt on the plains and pervasively altered basalt in the Columbia Hills. *Journal of Geophysical Research: Planets*, 111(2). doi: 10.1029/2005JE002584

Morris, R.V., Vaniman, D.T., Blake, D.F., Gellert, R., Chipera, S.J., Rampe, E.B., et al. (2016). Silicic volcanism on Mars evidenced by tridymite in high-SiO_2 sedimentary rock at Gale crater. *Proceedings of the National Academy of Science USA*, 113(26), 7071-7076. doi: 10.1073/pnas.1607098113.

Morrison, S. M., Downs, R. T., Blake, D. F., Vaniman, D. T., Ming, D. W., Hazen, R. M., et al. (2018). Crystal chemistry of martian minerals from Bradbury Landing through Naukluft Plateau, Gale crater, Mars. *American Mineralogist*, 103(6), 857-871. doi: 10.2138/am-2018-6124

Nachon, M., Clegg, S.M., Mangold, N., Schröder, S., Kah, L.C., Dromart, G., et al. (2014). Calcium sulfate veins characterized by ChemCam/Curiosity at Gale crater, Mars. *Journal of Geophysical Research: Planets*, 119(9), 1991-2016. doi: 10.1002/2013je004588.

Nachon, M., Mangold, N., Forni, O., Kah, L.C., Cousin, A., Wiens, R.C., et al. (2017) Chemistry of diagenetic features analyzed by ChemCam at Pahrump Hills, Gale crater, Mars. *Icarus*, 281, 121-136. doi: 10.1016/j.icarus.2016.08.026.

Novák, I., & B. Číčel (1978). Dissolution of smectites in hydrochloric acid: II. Dissolution rate as a function of crystallochemical composition. *Clays and Clay Minerals*, 26(5), 341-344. doi: 10.1346/ccmn.1978.0260504

Payré, V., K. L. Siebach, R. Dasgupta, A. Udry, E. B. Rampe, & S. M. Morrison (2020). Constraining Ancient Magmatic Evolution on Mars Using Crystal Chemistry of Detrital Igneous Minerals in the Sedimentary Bradbury Group, Gale Crater, Mars. *Journal of Geophysical Research: Planets*, 125(8). doi: 10.1029/2020je006467

Pettijohn, F. J., Potter, P. E. & Siever, R. (1987) *Sand and Sandstone, 2nd Ed.*, New York, NY: Springer-Verlag.

Post, J. L. (1984). Saponite from Near Ballarat, California. *Clays and Clay Minerals*, 32(2), 147-153. doi: 10.1346/ccmn.1984.0320209

Ramirez, R.M., & Craddock, R.A. (2018). The geological and climatological case for a warmer and wetter early Mars. *Nature Geoscience*, 11(4), 230-237. doi: 10.1038/s41561-018-0093-9

Rampe, E.B., Ming, D.W., Blake, D.F., Bristow, T.F., Chipera, S.J., Grotzinger, J.P., et al. (2017). Mineralogy of an ancient lacustrine mudstone succession from the Murray formation, Gale crater, Mars. *Earth and Planetary Science Letters*, 471, 172-185. doi: 10.1016/j.epsl.2017.04.021

Rampe, E.B., Blake, D.F., Bristow, T.F, Ming, D.W., Vaniman, D.T., Morris, R.V., et al. (2020a). Mineralogy and geochemistry of sedimentary rocks and eolian sediments in Gale crater, Mars: A review after six Earth years of exploration with Curiosity. *Geochemistry*. https://doi.org/10.1016/j.chemer.2020.125605

Rampe, E.B., Bristow, T.F., Morris, R.V., Morrison, S.M., Achilles, C.N., Ming, D.W., et al. (2020b). Mineralogy of Vera Rubin Ridge from the Mars Science Laboratory CheMin Instrument. *Journal of Geophysical Research: Planets*. doi: 10.1029/2019JE006306

Rasmussen, B., Krapež, B., Muhling, J. R., & Suvorova, A. (2015). Precipitation of iron silicate nanoparticles in early Precambrian oceans marks Earth's first iron age. *Geology*, 43(4), 303-306. doi: 10.1130/g36309.1

Rice, M.S., Gupta, S., Treiman, A. H., Stack, K.M., Calef, F., Edgar, L.A., et al. (2017). Geologic overview of the Mars Science Laboratory rover mission at the Kimberley, Gale crater, Mars. *Journal of Geophysical Research: Planets*, 122(1), 2-20. doi: 10.1002/2016je005200

Rivera-Hernández, F., Sumner, D. Y., Mangold, N., Banham, S. G., Edgett, K. S., Fedo, C. M., et al. (2020). Grain size variations in the Murray formation: Stratigraphic evidence for changing depositional environments in Gale crater, Mars. *Journal of Geophysical Research: Planets*, 125(2). doi: 10.1029/2019je006230

Rodgers, K. A., Browne, P. R. L., Buddle, T. F., Cook, K. L., Greatrex, R. A., Hampton, W. A., et al. (2004). Silica phases in sinters and residues from geothermal fields of New Zealand. *Earth-Science Reviews*, 66(1-2), 1-61. doi: 10.1016/j.earscirev.2003.10.001

Rutledge, A. M., Horgan, B. H. N., Havig, J. R., Rampe, E. B., Scudder, N. A., & Hamilton, T. L. (2018). Silica Dissolution and Precipitation in Glaciated Volcanic Environments and Implications for Mars. *Geophysical Research Letters*, 45(15), 7371-7381. doi: 10.1029/2018gl078105

Salvatore, M. R., Mustard, J. F., Head, J. W., Cooper, R. F., Marchant, D. R., & Wyatt, M. B. (2013). Development of alteration rinds by oxidative weathering processes in Beacon Valley, Antarctica, and implications for Mars. *Geochimica et Cosmochimica Acta*, 115, 137-161.

Salvatore, M., Truitt, K., Roszell, K., Lanza, N., Rampe, E., Mangold, N., et al. (2019). Investigating the role of anhydrous oxidative weathering on sedimentary rocks in the Transantarctic Mountains and implications for the modern weathering of sedimentary lithologies on Mars, Icarus, 319, 669-684. doi: 10.1016/j.icarus.2018.10.007

Scholle, P. A., & D. Ulmer-Scholle (2003). Cements and cementation. In G.V. Middleton, M.J. Church, M. Coniglio, L.A. Hardie, & F.J. Longstaffe (Eds.) *Encyclopedia of Sediments and Sedimentary Rocks*. Encyclopedia of Earth Sciences Series. Springer, Dordrecht. https://doi.org/10.1007/978-1-4020-3609-5_40

Siebach, K. L., Grotzinger, J. P., Kah, L. C., Stack, K. M., Malin, M., Léveillé, R., et al. (2014). Subaqueous shrinkage cracks in the Sheepbed mudstone: Implications for early fluid diagenesis, Gale crater, Mars. *Journal of Geophysical Research: Planets*, 119(7), 1597-1613.

Siebach, K. L., Baker, M. B., Grotzinger, J. P., McLennan, S. M., Gellert, R., Thompson, L. M., & Hurowitz, J. A. (2017). Sorting out compositional trends in sedimentary rocks of the Bradbury group (Aeolis Palus), Gale crater, Mars. *Journal of Geophysical Research: Planets*, 122(2), 295-328. doi: 10.1002/2016je005195

Siever, R. (1959) Petrology and geochemistry of silica cementation in some Pennsylvanian sandstones. In H. A. Ireland (Ed.), *Silica in Sediments* (special publication no. 7), Tulsa, OK: SEPM Society for Sedimentary Geology. https://doi.org/10.2110/pec.59.01.0055

Siever, R. (1983). Burial history and diagenetic reaction kinetics. *American Association of Petroleum Geology Bulletin*, 67, 684-691.

Smith, R.J., Rampe, E.B., Horgan, B.H.N., Dehouck, E., & Morris, R.V. (2017). The composition of secondary amorphous phases under different environmental conditions. Paper presented at the AGU Fall Meeting, New Orleans, LA.

Smith, R.J., Rampe, E.B., Horgan, B.H.N., & Dehouck, E. (2018). Deriving Amorphous Component Abundance and Composition of Rocks and Sediments on Earth and Mars. *Journal of Geophysical Research: Planets*, 123(10), 2485-2505. doi: 10.1029/2018je005612

Smith, R. (2021). Gale crater X-ray amorphous components - Supplemental materials [data set]. Mendeley, V3. doi: 10.17632/srm3v7sr76.3

Squyres, S. W., Arvidson, R. E., Ruff, S., Gellert, R., Morris, R. V., Ming, D. W., et al. (2008). Detection of silica-rich deposits on Mars. *Science*, 320(5879), 1063-1067. doi: 10.1126/science.1155429

Stack, K.M., Grotzinger, J.P., Kah, L.C., Schmidt, M.E., Mangold, N., Edgett, K.S., et al. (2014). Diagenetic origin of nodules in the Sheepbed member, Yellowknife Bay formation, Gale crater, Mars. *Journal of Geophysical Research: Planets*, 119(7), 1637-1664. doi: 10.1002/2014je004617.

Stack, K.M., Grotzinger, J.P., Lamb, M.P., Gupta, S., Rubin, D.M., Kah, L.C., et al. (2019). Evidence for plunging river plume deposits in the Pahrump Hills member of the Murray formation, Gale crater, Mars. *Sedimentology*, 66(5), 1768-1802. doi: 10.1111/sed.12558

Steefel, C.I., & Van Cappellen, P. (1990). A new kinetic approach to modeling water-rock interaction: The role of nucleation, precursors, and Ostwald ripening. *Geochimica et Cosmochimica Acta*, 54(10), 2657-2677. doi: 10.1016/0016-7037(90)90003-4

Stein, N., Grotzinger, J.P., Schieber, J., Mangold, N., Hallet, B., Newsom, H., et al. (2018). Desiccation cracks provide evidence of lake drying on Mars, Sutton Island member, Murray formation, Gale Crater. *Geology*, 46(6), 515-518. doi: 10.1130/g40005.1

Sun, V.Z., & Milliken, R.E. (2018). Distinct Geologic Settings of Opal‐A and More Crystalline Hydrated Silica on Mars. *Geophysical Research Letters*, 45(19), 10,221-210,228. doi: 10.1029/2018gl078494.

Sun, V.Z., Stack, K.M., Kah, L.C., Thompson, L., Fischer, W., Williams, A.J., et al. (2019). Late-stage diagenetic concretions in the Murray formation, Gale crater, Mars. *Icarus*, 321, 866-890. doi: 10.1016/j.icarus.2018.12.030

Sutter, B., McAdam, A.C., Mahaffy, P.R., Ming, D.W., Edgett, K.S., Rampe, E.B., et al. (2017). Evolved gas analyses of sedimentary rocks and eolian sediment in Gale Crater, Mars: Results of the Curiosity rover's sample analysis at Mars instrument from Yellowknife Bay to the Namib Dune. *Journal of Geophysical Research: Planets*, 122(12), 2574-2609. doi: 10.1002/2016je005225

Tarnas, J.D., Mustard, J.F., Lin, H., Goudge, T.A., Amador, E.S., Bramble, M.S., et al. (2019). Orbital Identification of Hydrated Silica in Jezero Crater, Mars. *Geophysical Research Letters*, 46(22), 12771-12782. doi: 10.1029/2019gl085584

Taylor, S., & McLennan, S. (2009). *Planetary Crusts: Their Composition, Origin and Evolution* (Cambridge Planetary Science). Cambridge: Cambridge University Press. doi:10.1017/CBO9780511575358

Thomson, B.J., Bridges, N.T., Milliken, R., Baldridge, A., Hook, S.J., Crowley, J.K., et al. (2011). Constraints on the origin and evolution of the layered mound in Gale Crater, Mars using Mars Reconnaissance Orbiter data. *Icarus*, 214(2), 413-432. doi: 10.1016/j.icarus.2011.05.002

Thompson, L. M., Berger, J. A., Spray, J. G., Fraeman, A. A., McCraig, M. A., O'Connell-Cooper, C. D., et al. (2020). APXS-Derived Compositional Characteristics of Vera Rubin Ridge and Murray Formation, Gale Crater, Mars: Geochemical Implications for the Origin of the Ridge. *Journal of Geophysical Research: Planets*, 125(10), e2019JE006319. doi: https://doi.org/10.1029/2019JE006319

Thorpe, M.T., Hurowitz, J.A., & Dehouck, E. (2019). Sediment geochemistry and mineralogy from a glacial terrain river system in southwest Iceland. *Geochimica et Cosmochimica Acta*, 263, 140-166. doi: 10.1016/j.gca.2019.08.003

Tosca, N.J., & Knoll, A.H. (2009). Juvenile chemical sediments and the long term persistence of water at the surface of Mars. *Earth and Planetary Science Letters*, 286(3-4), 379-386. doi: 10.1016/j.epsl.2009.07.004

Tosca, N. J., Ahmed, I. A. M., Tutolo, B. M., Ashpitel, A., & Hurowitz, J. A. (2018). Magnetite authigenesis and the warming of early Mars. *Nature Geoscience*, 11(9), 635-639. doi: 10.1038/s41561-018-0203-8

Treiman, A.H., Morris, R.V., Agresti, D.G., Graff, T.G., Achilles, C.N., Rampe, E.B., et al. (2014). Ferrian saponite from the Santa Monica Mountains (California, U.S.A., Earth): Characterization as an analog for clay minerals on Mars with application to Yellowknife Bay in Gale Crater. *American Mineralogist*, 99(11-12), 2234-2250. doi: 10.2138/am-2014-4763

Treiman, A. H., Bish, D. L., Vaniman, D. T., Chipera, S. J., Blake, D. F., Ming, D. W., et al. (2016). Mineralogy, provenance, and diagenesis of a potassic basaltic sandstone on Mars: CheMin X-ray diffraction of the Windjana sample (Kimberley area, Gale Crater). *Journal of Geophysical Research: Planets*, 121(1), 75-106. doi: 10.1002/2015JE004932

Tu, V.M., Hausrath, E.M., Tschauner, O., Iota, V., & Egeland, G.W. (2014). Dissolution rates of amorphous Al- and Fe-phosphates and their relevance to phosphate mobility on Mars. *American Mineralogist*, 99 (7): 1206–1215. doi: https://doi.org/10.2138/am.2014.4613

Vaniman, D.T., Bish, D.L., Ming, D.W., Bristow, T.F., Morris, R.V., Blake, D.F., et al. (2014). Mineralogy of a mudstone at Yellowknife Bay, Gale crater, Mars. *Science*, 343(6169), 1243480. doi: 10.1126/science.1243480

Watkins, J., Grotzinger, J., Stein, N., Banham, S. G., Gupta, S., Rubin, D., Stack, K. M., & Edgett, K. S. (2016). Paleotopography of erosional unconformity, base of Stimson Formation, Gale crater, Mars. Paper presented at 47th Lunar and Planetary Science Conference, Houston, TX.

Williams, R. M., Grotzinger, J. P., Dietrich, W. E., Gupta, S., Sumner, D. Y., Wiens, R. C., et al. (2013). Martian fluvial conglomerates at Gale crater. *Science*, 340(6136), 1068-1072. doi: 10.1126/science.1237317

Worden, R.H., & Burley, S.D. (2003), Sandstone Diagenesis: The Evolution of Sand to Stone. In R.H. Worden & S.D. Burley (Eds), *Sandstone Diagenesis: Recent and Ancient*, 1-44. doi: 10.1002/9781444304459.ch

Wordsworth, R. D. (2016). The Climate of Early Mars. *Annual Review of Earth and Planetary Sciences*, 44(1), 381-408. doi: 10.1146/annurev-earth-060115-012355

Yen, A.S., Ming, D.W., Vaniman, D.T., Gellert, R., Blake, D.F., Morris, R.V., et al. (2017). Multiple stages of aqueous alteration along fractures in mudstone and sandstone strata in Gale Crater, Mars. *Earth and Planetary Science Letters*, 471, 186-198. doi: 10.1016/j.epsl.2017.04.033

Yen, A.S., Morris, R.V., Ming, D.W., Schwenzer, S.P., Sutter, B., Vaniman, D.T., et al. (2020). Formation of tridymite and evidence for a hydrothermal history at Gale crater, Mars. *Journal of Geophysical Research: Planets*. doi: 10.1029/2020je006569